Journal of Theoretical Biology 255 (2008) 152–161

Contents lists available at ScienceDirect

Journal of Theoretical Biology

journal homepage: www.elsevier.com/locate/yjtbi

Generalizing Levins metapopulation model in explicit space: Models of intermediate complexity

Manojit Roy [a,*], Karin Harding [b], Robert D. Holt [a]

[a] Department of Zoology, University of Florida, 223 Bartram Hall, P.O. Box 118525, Gainesville, FL 32611-8525, USA
[b] Department of Marine Ecology, Gothenburg University, Box 461, S-405 30 Gothenburg, Sweden

ARTICLE INFO

Article history:
Received 8 May 2008
Received in revised form
16 July 2008
Accepted 18 July 2008
Available online 22 July 2008

Keywords:
Allee effect
Rescue effect
Anti-rescue effect
Spatial clustering
Power law
Range limit

ABSTRACT

A recent study [Harding and McNamara, 2002. A unifying framework for metapopulation dynamics. Am. Nat. 160, 173–185] presented a unifying framework for the classic Levins metapopulation model by incorporating several realistic biological processes, such as the Allee effect, the Rescue effect and the Anti-rescue effect, via appropriate modifications of the two basic functions of colonization and extinction rates. Here we embed these model extensions on a spatially explicit framework. We consider population dynamics on a regular grid, each site of which represents a patch that is either occupied or empty, and with spatial coupling by neighborhood dispersal. While broad qualitative similarities exist between the spatially explicit models and their spatially implicit (mean-field) counterparts, there are also important differences that result from the details of local processes. Because of localized dispersal, spatial correlation develops among the dynamics of neighboring populations that decays with distance between patches. The extent of this correlation at equilibrium differs among the metapopulation types, depending on which processes prevail in the colonization and extinction dynamics. These differences among dynamical processes become manifest in the spatial pattern and distribution of "clusters" of occupied patches. Moreover, metapopulation dynamics along a smooth gradient of habitat availability show significant differences in the spatial pattern at the range limit. The relevance of these results to the dynamics of disease spread in metapopulations is discussed.

1. Introduction

The role of space in ecological dynamics and organization is a fundamental topic in the ecological sciences (Holt, 1993; Tilman and Kareiva, 1997). Metapopulation theory, proposed by Levins (1969) and subsequently studied by many others in both real and model systems (Hanski, 1999; Hanski and Gaggiotti, 2004), highlights the importance of the spatial process of dispersal in sustaining species inhabiting patchy habitats. In its simplest form, metapopulation dynamics involve balancing stochastic extinction on a patch with colonization from other occupied patches, which facilitates population persistence regionally even in the face of repeated local extinctions. The simplicity of Levins' model makes it mathematically tractable, but at the same time susceptible to criticism because of its lack of realism (for example, Harrison and Taylor, 1997). This has prompted the birth of a large number of metapopulation models with differing degrees of complexity.

In parallel with the development of increasingly complex models tailored to specific ecological systems (Hanski and Gaggiotti, 2004), conceptual models have also emerged that study the effects of improving the assumptions about colonization and extinction dynamics within the basic Levins framework (Harding and McNamara, 2002; Ellner and Fussmann, 2003). Harding and McNamara (2002) presented a unifying framework for the Levins model by incorporating several realistic biological processes, such as Allee effect, Rescue effect and Anti-rescue effect, via appropriate modifications of the two basic functions of colonization and extinction rates. They showed that such modifications can fundamentally alter the predictions of Levins model, for example, by introducing unstable equilibria (for both the Allee and Rescue effects), and also decreasing (stable) equilibrial occupancy with increasing emigration rate (in the Anti-rescue effect).

However, Harding and McNamara (2002) assumed global dispersal, that is, individuals are assumed to disperse uniformly all over the landscape (as in Levins model). Most real individuals, by contrast, move to a more limited extent from their natal patch, particularly given that movement can be restricted by resource availability, territoriality, predation risk, and so on. In this paper, we incorporate such limited movements onto the basic Levins model in a spatially explicit framework. We modify the colonization

* Corresponding author. Tel.: +1 352 392 1040; fax: +1 352 392 3704.
E-mail addresses: roym@ufl.edu (M. Roy), karin.harding@marbot.gu.se (K. Harding), rdholt@zoo.ufl.edu (R.D. Holt).

0022-5193/$ - see front matter © 2008 Elsevier Ltd. All rights reserved.
doi:10.1016/j.jtbi.2008.07.022

and extinction processes by incorporating Allee, Rescue and Anti-rescue effects as in Harding and McNamara (2002), but with the processes operating within local neighborhoods. Our goal is to study how metapopulation dynamics, captured by the overall (landscape-wide) colonization and extinction rates, are influenced by these local processes, which in turn affect the equilibrial patch occupancy and other features of the species distribution in space.

Because of localized dispersal, spatial correlation is expected to develop among the dynamics of neighboring populations, a correlation that decays with distance between patches. The extent of this correlation at equilibrium should differ among metapopulations, depending on which local processes prevail in the colonization and extinction dynamics. Because Allee and Rescue effects can facilitate patch occupancy via neighborhood dispersal, one expects these metapopulations to have a larger range of spatial correlation at equilibrium, compared to both the standard Levins and the Anti-rescue metapopulation. We show that these differences influence the spatial pattern and distribution of "clusters" of occupied patches. Moreover, metapopulation dynamics along a smooth gradient of habitat availability can show significant differences at range limits, reflecting these local processes.

2. Basic Levins metapopulation model

In the classic Levins metapopulation model (Levins, 1969), individuals disperse globally and colonizers arrive on a patch at an "arrival rate" $A = m(N/L) = mp$ (we assume no mortality during movement), where m is the per-patch emigration rate from occupied patches, N is the number of occupied patches in a landscape of size L, and $p = N/L$ thus gives the fraction of occupied patches. A successful colonization occurs only if the focal patch is empty, the probability of which is $1-p$. Therefore, the overall (metapopulation-level) colonization rate is $C_{Levins} = A(1-p) = mp(1-p)$. The overall extinction rate is $E = ep$, where e is the per-patch extinction rate. The metapopulation dynamics then follows the familiar equation

$$\frac{dp}{dt} = C_{Levins} - E = mp(1-p) - ep. \quad (1)$$

The metapopulation persists indefinitely at the (globally stable) equilibrial occupancy $p^* = 1 - e/m$, which corresponds to the point of intersection between C_{Levins} (broken curved line in Fig. 1A) and E (broken diagonal line). Keeling (2002) explored a stochastic version of Eq. (1), and also compared the C_{Levins} and E plots (in Fig. 1A) with a metapopulation incorporating stochastic subpopulation dynamics.

2.1. Levins metapopulation with neighborhood colonization (LNC)

In the idealized scenario of the Levins model, colonizers in any given empty patch arrive uniformly from all over the landscape. In reality, however, the dispersal distance of an individual is constrained by the range of its movements, and is often spatially restricted to a small neighborhood of its natal patch. We explicitly modeled such localized colonization on a regular grid, each site of which represents a habitat patch, and where emigrants from an occupied patch disperse only to the z neighboring patches. In this Levins metapopulation model with neighborhood colonization (hereafter referred to as "LNC", to distinguish it from the global model, denoted simply by "Levins"), the arrival rate at a patch i is given as $A_i = mn_i/z$, where n_i is the number of occupied neighbors of the focal patch ($0 \leqslant n_i \leqslant z$, and $n_i/z \to p$ as $z \to L$). Successful

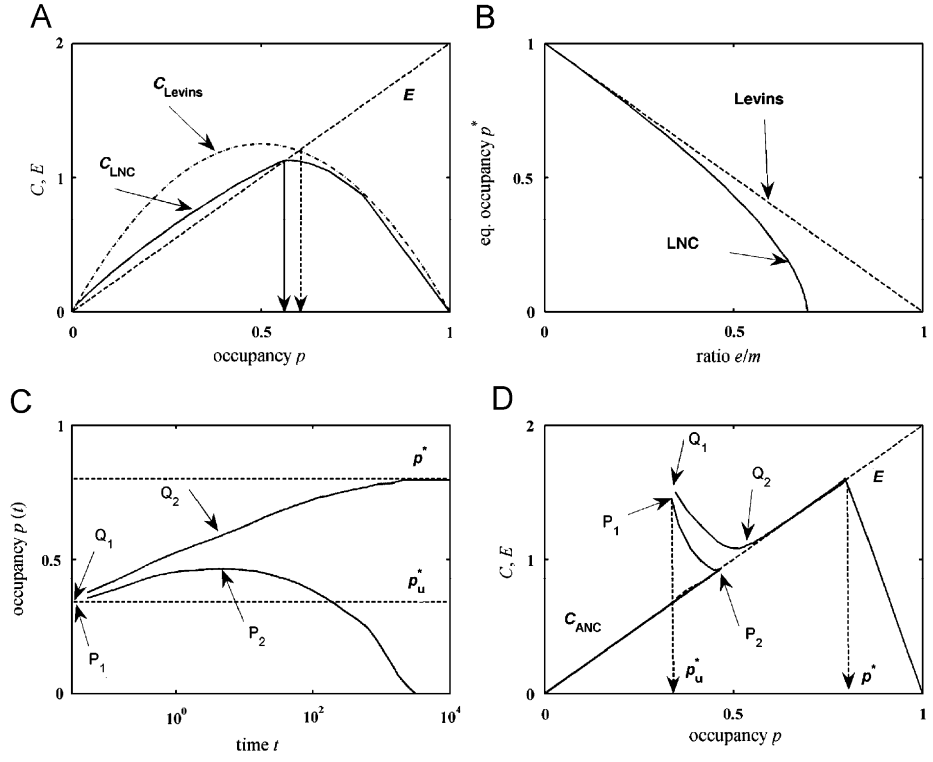

Fig. 1. (A) Colonization rates are plotted against patch occupancy p for the LNC model with $z = 8$ (solid line) and the global Levins model (broken line). Extinction rate $E = ep$ is same in both models (broken diagonal line). The downward vertical arrows denote the corresponding equilibrial occupancy p^*. Model parameter values chosen are $m = 5$ and $e = 2$. (B) Equilibrial occupancy p^* is plotted against the ratio e/m for the LNC (solid line) and Levins (broken line) models. For the horizontal axis we fix $m = 5$ and vary e from 0 to 5. (C) Occupancy time-series plots $p(t)$ for the ANC model with $z = 8$ are shown starting with two initial occupancies 0.332 and 0.338, near and on either side of the unstable equilibrium $p_u^* = 0.335$ (note the logarithmic horizontal axis). (D) Corresponding colonization rate C_{ANC} and extinction rate E are plotted against p (see text for details). Model parameters used are $m = 8$ and $e = 2$.

colonization of the patch i requires it to be empty, and the overall colonization rate C_{LNC} is thus computed by averaging A_i over all empty patches, multiplied by the probability $1-p$ that the focal patch is empty: $C_{LNC} = \langle A\rangle_e(1-p) = (m/z)\langle n\rangle_e(1-p)$, where $\langle\ \rangle_e$ denotes spatial averaging over all empty patches in the metapopulation (computed numerically). The extinction rate is $E = ep$, the same as in the global model (i.e., extinction of an occupied patch does not depend on the state of other patches). The dynamics of the LNC model is then given by

$$\frac{dp}{dt} = C_{LNC} - E = \frac{m}{z}\langle n\rangle_e(1-p) - ep. \tag{2}$$

For global colonization ($z\to L$), we have $\langle n\rangle_e/z = p$, and Eq. (2) reduces to Eq. (1).

We note that the simplest LNC model with $z = 4$ is same as the well-known "contact process" model, which was originally introduced by Harris (1974), and later studied extensively in ecology (see, for example, Durrett and Levin, 1994; Levin and Pacala, 1997; Snyder and Nisbet, 2000; Ovaskainen et al., 2002; Oborny et al., 2005), epidemiology (Levin and Durrett, 1996; Holmes, 1997), and statistical physics (Marro and Dickman, 1999; Hinrichsen, 2000). There is also a rich literature on the analysis of similar models using pair-correlation approximations (or PCA) (Sato and Iwasa, 2000, and references therein; Hui and Li, 2004). Our purpose of reintroducing this well-studied system here is to use it as a springboard to build a series of realistic model extensions, and to explore the effects of various local processes on the shape of the overall colonization and extinction rates (in the spirit of Harding and McNamara, 2002), which in turn will influence the equilibrial properties and spatial distribution patterns, as we shall see below.

Numerical details of implementing the LNC model, and computing C_{LNC} and E, are relegated to Appendix A. As shown in Fig. 1A, localized dispersal lowers the colonization rate, especially at low patch occupancy levels, compared to the global dispersal, that is, $C_{LNC} < C_{Levins}$ (the extinction rate E is same in both models). The low colonization rate in turn reduces the equilibrial occupancy p^* (solid vertical arrow in Fig. 1A). Fig. 1B shows how p^* changes with the ratio e/m in the LNC model. The predicted Levins equilibrium $p^* = 1 - e/m$ is also shown (dashed diagonal line) for comparison. The departure of the two graphs at high e/m is due to the increasing importance of spatially localized correlations in the LNC dynamics, which are absent in the global model. The PCA technique includes pair-wise correlations, and provides a closer fit to the LNC model (see Fig. 18.3 in Sato and Iwasa, 2000). The PCA graph still deviates from the LNC graph at higher e/m values: at larger rates of local extinction, there is a high degree of clumping of occupied patches (because of neighborhood colonization) as they become rare, and the triplet and higher-order correlations (ignored in the PCA model) become increasingly significant (Sato and Iwasa, 2000).

3. Extensions of the basic metapopulation model

In the basic metapopulation models described above, colonization of an empty patch is determined by an arrival rate that increases simply with the proportion of occupied patches (either in the neighborhood or everywhere). Moreover, the extinction of an occupied patch occurs at a constant rate, independent of the surrounding occupancy level. These assumptions simplify the analysis, but they do exclude a range of realistic and widespread biological phenomena. For example, successful colonization may depend on the establishment of a certain minimum population size in the local neighborhood, which implies a departure of overall colonization rates from the simple linear dependence on patch occupancy. Furthermore, occupancy of neighboring patches should alter the influx rate of immigrants into a focal occupied patch, which can in turn have either positive or negative effects on that patch's extinction risk. Below we consider some of these realistic extensions—Allee effects, Rescue effects, and Anti-rescue effects—of the basic metapopulation dynamics in explicit space.

3.1. Metapopulation model with an Allee effect

The "Allee effect" was named after Allee (1931, 1938) who emphasized the positive effects of associating with conspecifics. Odum (1953) extended the scope of this term to include the negative effects for a population of being at very low densities (also see Courchamp et al., 1999; Stephens et al., 1999). An Allee effect can drive small isolated populations to extinction, for instance due to a decline in reproductive opportunities (Dennis, 1989; Lewis and Kareiva, 1993; McCarthy, 1997; Hurford et al., 2006). Allee effects can also influence dynamics at the metapopulation scale. For example, dispersal limitations that occur when patch occupancy is low can reduce the arrival rate of colonizers to an empty patch. Given this low density, an Allee effect (at the within-patch scale) can then prevent the small (immigrant) population from establishing on the patch (Amarasekare, 1998; Keitt et al., 2001). Harding and McNamara (2002) showed that such non-linear density dependence in colonization success leads to an unstable equilibrium for patch occupancy; metapopulations below this equilibrium do not persist, whereas those above it persist often at a high equilibrium.

Because dispersal in real metapopulations is spatially restricted, the Allee effect observed in the focal patch i should clearly depend on the number of its occupied neighbors, n_i. Several studies have examined the impacts of such localized Allee effect on, for example, invasion success (Keitt et al., 2001), metapopulation complexity and distribution (Hui and Li, 2003, 2004), and regional extinction (Windus and Jensen, 2007). As an example of a neighborhood formulation of an Allee effects in a metapopulation model (hereafter called "ANC"), we choose a simple threshold-type dependence of the local arrival rate on n_i:

$$A_i(n_i) = \begin{cases} 0 & \text{if } n_i < z/2, \\ m & \text{if } n_i \geqslant z/2, \end{cases} \tag{3}$$

(replacing $A_i = mn_i/z$ in the LNC model). The metapopulation colonization rate is computed as $C_{ANC} = \langle A\rangle_e(1-p)$, as before. Such a threshold function mimics an Allee effect on a local scale, in that the colonization of the focal patch is successful only if the number of occupied neighbors exceeds a certain minimum value.

For the parameter values used in our example, the dynamics exhibit an unstable equilibrium of $p_u^* = 0.335$ (see Appendix A for a method of computing this equilibrium) and a stable equilibrium of $p^* = 0.8$. Fig. 1C shows examples of two occupancy time series $p(t)$ starting with closely placed initial occupancies, $p(0) = 0.332$ and 0.338, on either side of the unstable point p_u^* (denoted by labels P_1 and Q_1, respectively). A logarithmic horizontal axis is used to highlight the early transient patterns. As expected, the metapopulation starting at Q_1 stabilizes at the equilibrial occupancy p^* after a fairly long transient, whereas the one starting at P_1 initially follows the upper trajectory (because of the closeness of the initial points), but eventually turns around, and the metapopulation then becomes extinct. The segments (P_1,P_2) and (Q_1,Q_2) in the two time series correspond to those in C_{ANC} in Fig. 1D (see below).

Fig. 1D shows the colonization rate C_{ANC} and extinction rate E for this model (see Appendix A for the method of computing them). Because of the unstable point p_u^*, from which trajectories

diverge away (to either 0 or p^*), C_{ANC} has a discontinuity at $p = p_u^*$ (shown by the vertical broken arrow on the left). The two segments (P_1,P_2) and (Q_1,Q_2) in C_{ANC} are the results of transient dynamics (see Appendix A), and they bracket the same ranges of p values as the corresponding time series segments in Fig. 1C. The functions C_{ANC} and E lie very close to each other within most of the range $0 \leqslant p \leqslant p^*$, and their intersection near the point of departure gives the stable equilibrium p^* (vertical broken arrow on the right in Fig. 1D).

3.2. Metapopulation model with a Rescue effect

In the Allee metapopulation above, the colonization success of an empty patch depends non-linearly on the occupancy of neighboring patches, whereas the extinction of an occupied patch is assumed to be entirely a within-patch event, independent of the state of other patches (as in the original Levins model). However, immigration from other occupied patches in the landscape can sometimes reduce the extinction risk of dwindling subpopulations—an effect known as the "Rescue effect" (Brown and Kodric-Brown, 1977). Harding and McNamara (2002) included the Rescue effect in the Levins metapopulation by assuming the (per-patch) extinction rate to be a non-linear decreasing function of p, and showed the presence of an unstable equilibrium p_u^*, similar to that which occurs given the Allee effect.

Incorporating a Rescue effect in an explicit-space metapopulation model with localized dispersal can generate interesting spatio-temporal patterns (Keymer et al., 1998), and also stabilize the overall metapopulation dynamics (Hui and Li, 2003). To illustrate a neighborhood formulation of a Rescue metapopulation (hereafter called "RNC"), we choose a threshold-type dependence of the local per-patch extinction rate f_i on n_i:

$$f_i(n_i) = \begin{cases} e & \text{if } n_i < z/2, \\ e/10 & \text{if } n_i \geqslant z/2. \end{cases} \tag{4}$$

(By contrast, in the LNC and ANC models above, we assumed $f_i = e$ everywhere, irrespective of the neighborhood occupancy.) Expression (4) implements a simplified Rescue effect on a local scale: the risk of extinction of a local population decreases 10-fold if the neighborhood occupancy exceeds a certain minimum. The arrival rate A_i is assumed to be proportional to n_i, as in the LNC model, i.e., $A_i = mn_i/z$. The RNC metapopulation dynamics can then be written as

$$\frac{dp}{dt} = C_{RNC} - E_{RNC} = \frac{m}{z}\langle n\rangle_e(1-p) - \langle f\rangle_o p, \tag{5}$$

with f given by Eq. (4), and $\langle\ \rangle_o$ denoting spatial averaging over all occupied patches (the overall colonization rate C_{RNC} is the same as C_{LNC} in the LNC model). Note that in the RNC model, *both* colonization and extinction processes depend on neighborhood dispersal, unlike the LNC and ANC models, where extinction is strictly a within-patch process.

Fig. 2A shows examples of two metapopulation time series $p(t)$ starting with initial occupancies $p(0) = 0.441$ and 0.448 (labeled as P_1 and Q_1), respectively, below and above the unstable point $p_u^* = 0.445$ (for the parameters used). (The horizontal time axis is in log scale to highlight the transient patterns, as in Fig. 1C). As expected, the metapopulation with initial occupancy below p_u^* becomes extinct, and the one with initial occupancy above p_u^* settles at the higher stable equilibrium $p^* = 0.835$. However, in contrast to the example shown in the Allee model (Fig. 1C), the transient pattern of the persisting metapopulation first exhibits a declining occupancy, before the trajectory starts to go up and

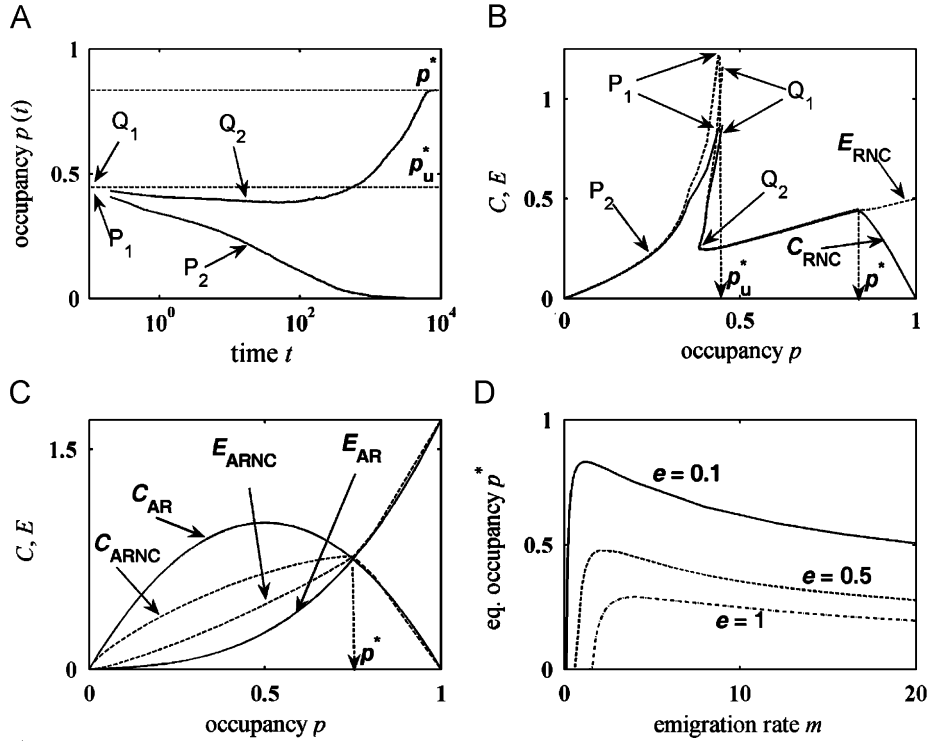

Fig. 2. (A) Occupancy time series $p(t)$ for the RNC model with $z = 8$ are shown starting with two initial occupancies 0.441 and 0.448 near the unstable equilibrium $p_u^* = 0.445$ (note the logarithmic horizontal axis). (B) Corresponding rates C_{RNC} and E_{RNC} are plotted against p (see text for details). Mode parameters used are $m = 3.5$ and $e = 5$. (C) Colonization and extinction rates of the global and neighborhood Anti-rescue metapopulation models are plotted on top of each other (solid line plots for the global model and broken line plots for the local model, respectively) (see text for model definitions). They both exhibit the same equilibrial occupancy $p^* = 0.75$. Model parameters are $m = 4$ and $e = 0.1$. (D) Changes of p^* are plotted against emigration rate m for three different values of e in the ARNC model.

eventually approaches p^*. This contrast reflects the effects of differing local processes of colonization and extinction on the initial build-up of spatial correlations in these two models.

Fig. 2B shows the corresponding colonization and extinction rates C_{RNC} and E_{RNC} (computed using similar steps as narrated in Appendix A for Fig. 1D), highlighting the two equilibria and the discontinuity near the unstable equilibrium p_u^*. The discontinuity now occurs in both C_{RNC} and E_{RNC}, unlike in the ANC model, in which the extinction rate $E = ep$ is a continuous straight line (compare the dashed line plot with that in Fig. 1D). Also note that the discontinuity in C_{RNC} arises despite the local arrival rate A_i having the same (smooth) expression as in the LNC model (which does not exhibit discontinuity): this discontinuity in C_{RNC} is driven by the one in E_{RNC}, which in turn results from the threshold function assumed in Eq. (4). [The transient segments (P_1,P_2) and (Q_1,Q_2) for both C_{RNC} and E_{RNC} (indicated by arrows in Fig. 2B) correspond to the segments in the two time series (in Fig. 2A), in the sense that they bracket the same ranges of p values.]

3.3. Metapopulation model with an Anti-rescue effect

In contrast to the Rescue effect, enhanced immigration can in some situations also significantly enhance the extinction risk of the focal population—an effect known as an "Anti-rescue effect" (Harding and McNamara, 2002). For example, immigrants can inject pathogens into the population, causing epidemic outbreaks that can depress population size (Grenfell et al., 1995; Grenfell and Harwood, 1997); increased gene flow can hinder the pace of local adaptation to variable environments (Hastings and Harrison, 1994; Rolán-Alvarez et al., 1997); high dispersal rate can induce synchronous fluctuations among subpopulations, thus increasing the extinction risk of the entire metapopulation (Earn et al., 2000; Roy et al., 2005); immigrants for social reasons may be precluded from reproduction by residents, but still use resources. A simple way to model an Anti-rescue effect in a globally dispersing metapopulation (hereafter called "AR") is to assume that the per-patch extinction rate $f(p)$ increases with p:

$$f(p) = e(1 + m^2p^2). \tag{6}$$

The metapopulation extinction rate is given by $E_{AR} = fp = ep(1+m^2p^2)$. The colonization rate is the same as in the (globally dispersing) Levins metapopulation: $C_{AR} = mp(1-p)$. The stable equilibrium $p^* = (\sqrt{4me - 4e^2 + 1} - 1)/(2me)$ is feasible if $m > e$. Thus, p^* is not a monotonically increasing function of the migration rate m, and it can in fact decrease with increasing m for large values of m (Harding and McNamara, 2002), in contrast to the other metapopulation models discussed above.

As an example of an Anti-rescue metapopulation model with neighborhood dispersal ("ARNC"), we use the following neighborhood version of Eq. (6) for the local extinction rate f_i

$$f_i(n_i) = e\left\lfloor 1 + (mn_i/z)^2 \right\rfloor. \tag{7}$$

As in the LNC (and RNC) metapopulation, we assume that the local arrival rate is $A_i = mn_i/z$. Thus, the ARNC dynamics is

$$\frac{dp}{dt} = C_{ARNC} - E_{ARNC} = m\frac{\langle n\rangle_e}{z}(1-p) - ep\left(1 + \frac{m^2\langle n^2\rangle_o}{z^2}\right), \tag{8}$$

where C_{ARNC} and E_{ARNC} are the colonization and extinction rates of ARNC metapopulation.

Fig. 2C overlays the colonization and extinction rates for global (solid lines) and neighborhood (broken lines) Anti-rescue models, showing their qualitative similarities. There is only one (stable) equilibrium p^*, which takes the same value 0.75 (for the parameters used) for both models. Thus, unlike the LNC model (Fig. 1A), localized dispersal in ARNC model does not lower p^*. Fig. 2D shows that p^* increases sharply with m for low levels of emigration, but then begins a slow decrease after m crosses a certain threshold that increases with e, broadly similar to the predictions of the global model (Harding and McNamara, 2002).

4. Spatial clustering analysis

Dispersal among neighboring patches is expected to generate spatially localized correlation in occupancy that decays with distance. Because of this spatial correlation, occupied patches tend to form self-organized aggregation or "clusters". Such self-organization in the dynamics of ecological systems is a topic of great interest (Rohani et al., 1997; Keymer et al., 1998; Pascual et al., 2002; Solé and Bascompte, 2006). We define a "cluster" as a group of occupied patches that are connected to each other via the 8 nearest neighbors (the same neighborhood that defines the dispersal radius—thus the connectivity is determined by the range of movements). A snapshot of the metapopulation at any given time exhibits a range of cluster sizes, from as small as a two-patch cluster (a single isolated patch is not considered a cluster) to as large as the order of the entire metapopulation size (depending on patch occupancy level).

Figs. 3A–D show examples of snapshots at stable equilibrium for the metapopulation models discussed here, where black pixels denote the distribution of occupied patches; the equilibrial patch occupancy is kept at $p^* = 0.4$ in all these plots. This occupancy level is slightly below the so-called "percolation point" $p_P = 0.407$ in the classic Percolation model with 8 neighbor connectivity (Stauffer and Aharony, 1992; Guichard et al., 2002), at which a giant "spanning" cluster—that spans the grid from one edge to the other—appears as p is increased across p_P. Our choice of the occupancy level in Figs. 3A–D is designed to reveal patterns below that leading to a spanning cluster. Interestingly, one of these models has a percolation point less than 0.4, as we show below. For the clustering results in Fig. 3, we use the local arrival rate $A_i(n_i) = 1/[1 + \exp(-n_i + z/2)]$ and $A_i(0) = 0$ instead of Eq. (3) in the ANC model, and the local extinction rate $f_i(n_i) = 1/(1+n_i/z)$ instead of Eq. (4) in the RNC model. This is for illustrative purposes, because these smooth functions allow the equilibrial occupancy p^* to be as low as 0.4 in these two models; whereas with the step functions in Eqs. (3) and (4), p^* always stays at high values (>0.75) for all combinations of m and e. The LNC and ARNC models are the same as described earlier.

The degree of aggregation varies across these models, depending on the nature of the localized dispersal that drives the colonization and extinction processes. An eyeball comparison of the snapshots in Figs. 3A–D suggests that the Anti-rescue effect (ARNC model) generates the least amount of aggregation, whereas the Allee effect (ANC) generates the most, and the RNC and LNC snapshots lie in between. Both the Allee and Rescue effects enhance the local (spatial) correlation of occupied patches compared to the Levins model, whereas the Anti-rescue effect decreases the correlation (facilitates creation of more occupied-empty pairs) by increasing extinction risk in the presence of occupied neighbors. Thus, Fig. 3B shows large clusters, followed by Fig. 3C and A, and Fig. 3D shows mostly small clusters.

These observations can be quantified by estimating the average size $\bar{s}$ of these clusters, defined as $\bar{s} = \sum sn(s)/\sum n(s)$ where $n(s)$ denotes the number of clusters of size s, which gives a measure of the degree of aggregation (spatial correlation) in the system. For the four metapopulation models, we have $\bar{s}_{LNC} = 63$, $\bar{s}_{ANC} = 106$, $\bar{s}_{RNC} = 72$ and $\bar{s}_{ARNC} = 38$ (each of these estimates is computed by averaging over 500 independent snapshots on a 1000×1000

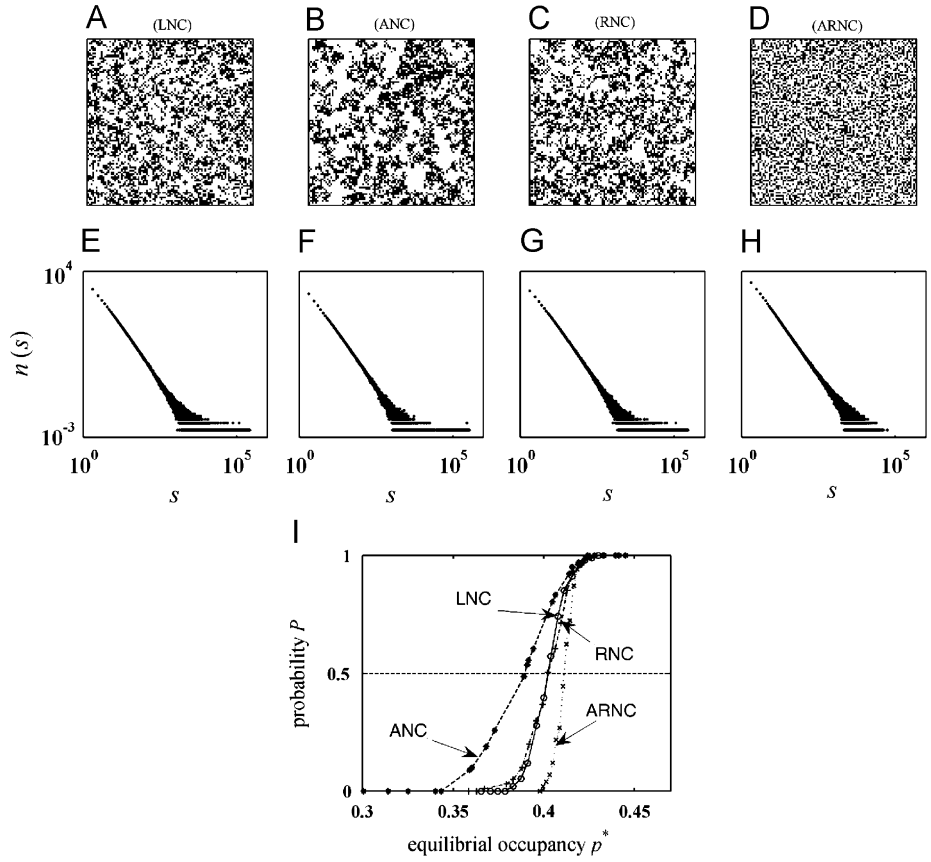

Fig. 3. (A–D) Examples of equilibrial snapshots are shown for the LNC, ANC, RNC and ARNC models (middle 150×150 segment of the 1000×1000 grid is plotted). Black and white pixels denote occupied and empty patches respectively. Equilibrial occupancy is set at $p^* = 0.4$ in all these examples (see text). Model parameters used are $m = 3.82$ and $e = 2$ (for LNC), $m = 5.23$ and $e = 2$ (for ANC), $m = 6.89$ and $e = 5$ (for RNC), and $m = 6.55$ and $e = 0.5$ (for ARNC). (E–H) Cluster size distributions corresponding to the snapshots in A–D are plotted on log–log scale (see text). Data for each cluster plot are obtained by averaging over 500 independent snapshots. (I) Percolation probability P (see text for definition) is plotted against the equilibrial occupancy p^* in the four models. The parameter e is kept fixed (at the magnitude stated above for each model), and m is varied to obtain the ranges of p^* in this plot.

grid). For comparison, the average cluster size for the Levins metapopulation with random (global) dispersal (which does not have any spatial correlation in the dynamics) is $\bar{s}_{Levins} = 42$. These estimates give the hierarchy $\bar{s}_{ARNC} < \bar{s}_{Levins} < \bar{s}_{LNC} < \bar{s}_{RNC} < \bar{s}_{ANC}$, which confirms our earlier qualitative observations.

Figs. 3E–H show the frequency distribution of these clusters on a log–log scale, by plotting the number $n(s)$ of clusters versus the size s. These distributions tend to follow a power-law distribution $n(s) \propto s^{-\beta}$, where the exponent β gives the slope of the straight line on the log–log plot. It is well-known from percolation studies that such a scale-free distribution of cluster sizes arises in grid-based models at the percolation point (Stauffer and Aharony, 1992), and similar patterns have also been reported in ecological models with neighborhood interactions (Pascual et al., 2002; Roy et al., 2003; Pascual and Guichard, 2005). Least-squared estimates of $\beta_{LNC} = \beta_{RNC} = 1.81$, and $\beta_{ARNC} = 1.8$ capture the slopes in the size range $20 \leqslant s \leqslant 2000$ for the respective plots with an $R^2 \geqslant 0.99$, implying that the power-law pattern does not depend significantly on the details of local dispersal in the dynamics. These estimates were obtained from the cumulative distribution plots $n(>s) \propto s^{-\alpha}$ to reduce the scatter at large cluster sizes, and by using the relationship $\beta = \alpha - 1$. (Note that even though the slopes are similar within the specified range of cluster sizes, differences do arise in the frequency of very small and very large clusters; for example, in the ARNC distribution plot in Fig. 3H, there are more small clusters and less large clusters than in the other plots, as expected.)

In Fig. 3I we illustrate the method of computing the percolation point in these models, by estimating the probability P that a snapshot (such as in Figs. 3A–D) has a spanning cluster, against the equilibrial occupancy level p^*. For each value of p^*, P is computed as the proportion of 200 independent snapshots that has a spanning cluster. (Note that p^* is not a model parameter; we vary the parameters m and e in each model to obtain the range of p^* values in Fig. 3I.) From the definition, P should rapidly rise from 0 to 1 as p^* is increased across the percolation point, and we numerically define the percolation point as that value of p^* at which $P = 0.5$. From Fig. 3I (the horizontal axis is blown up near $P = 0.5$ to highlight the differences in the plots), we estimate the percolation point in these models to be as follows: $p^*_{ANC} = 0.39$, $p^*_{LNC} = p^*_{RNC} = 0.402$, and $p^*_{ARNC} = 0.411$. These values are consistent with the earlier estimates of average cluster sizes, indicating again that the ANC model has the largest degree of spatial correlation (that lowers the occupancy level at which spanning clusters appear), whereas the ARNC model has the smallest.

The spanning cluster provides a globally connected pathway for an individual to move from one end of the metapopulation landscape to the other via neighborhood dispersal. A low percolation point, as in the ANC model, can thus facilitate persistence at somewhat lower occupancy, by allowing individuals to move large distances and avoid stochastic extinction. But, it can also cause harmful effects, for instance by promoting an infectious disease to spread over large scales in the metapopulation and endangering its persistence.

5. Metapopulations along gradients

The range limit of a species arises from variations in demographic processes, such as birth, death and migration, along an environmental gradient, for example in habitat quality, so that at the boundary the population growth rate changes from positive to negative (Wilson et al., 1996; Gaston, 2003; Holt et al., 2005). Studies have shown that such distributional limits can occur also from metapopulation dynamics, when the metapopulation is placed on a smooth environmental gradient (Lennon et al., 1997; Holt and Keitt, 2000). Using a discrete-time version of the LNC model, Holt and Keitt (2000) showed that mean occupancy along the gradient falls linearly when the gradient is in habitat availability, rather than in the colonization and extinction rates, where the range boundaries can be relatively sharp.

Here, we explore the habitat-gradient case with our continuous-time LNC model, and compare the resulting patterns with those generated by ANC, RNC and ARNC model dynamics (as defined above with the local per-patch rates Eqs. (3), (4) and (7) respectively). As in Holt and Keitt (2000), we assume that the fraction k of available suitable habitat decreases linearly from 1 to 0 along the x-axis from left to right, so that the LNC dynamics in Eq. (2) now becomes

$$\frac{dp}{dt} = C_{LNC}(x) - E = \frac{m}{z}\langle n\rangle_e[k(x) - p] - ep. \tag{9}$$

The colonization and extinction rate parameters, m and e, are assumed to be uniform across the metapopulation, as before. A patch can be occupied only if available, and thus it is in one of the three following states at any given time: available and occupied (black pixels in Figs. 4A–D), available and empty (gray pixels), or unavailable (white pixels).

Because the available habitat decreases from left to right, the overall colonization rate C_{LNC} also falls, and at some distance along the x-axis colonization fails to balance extinction, which then gives rise to the metapopulation range limit. However, because of the stochastic nature of the habitat (availability of a patch is determined by the probability $k(x)$), the species border itself is stochastic and fuzzy (Fig. 4A). As in Holt and Keitt (2000), mean occupancy $\langle p\rangle$, averaged over the vertical transect at each point along the x-axis, decreases linearly along the gradient, dropping to zero at about 90% habitat loss (the exact location of the range limit depends on the parameters used) (Fig. 4E). This pattern of linear decrease is due to the linear decrease in habitat availability $k(x)$ with increasing x. The fluctuation in the occupancy level, given by the standard deviation for $\langle p\rangle$, stays relatively flat along the gradient except near the range limit, where it falls (Fig. 4I). These fluctuations arise from repeated colonization and extinction events, due to the stochasticity inherent in both habitat availability and in metapopulation dynamics.

Comparing the range limits among the different metapopulation models (Figs. 4A–D), the Allee metapopulation (ANC) gives the sharpest range border (Fig. 4B) relative to the other models. For the parameters chosen, the mean occupancy $\langle p\rangle$ in the ANC model rapidly drops to zero even at about 35% habitat loss (Fig. 4F), and the standard deviation shows a sharp peak near the range limit (Fig. 4J; note the vertical range is almost an order of magnitude larger than in the other three plots). Both the pattern of sharp range border and large fluctuations at the border are due to the localized Allee effect (Eg. (3)) assumed in the model: as occupancy decreases along the gradient, at the range limit it falls below the threshold of local unstable equilibria, and patches that become extinct are not readily re-colonized, giving the sharp border. There is also a high degree of ephemeral clustering of occupied sites near the range limit (see Holt and Keitt, 2000),

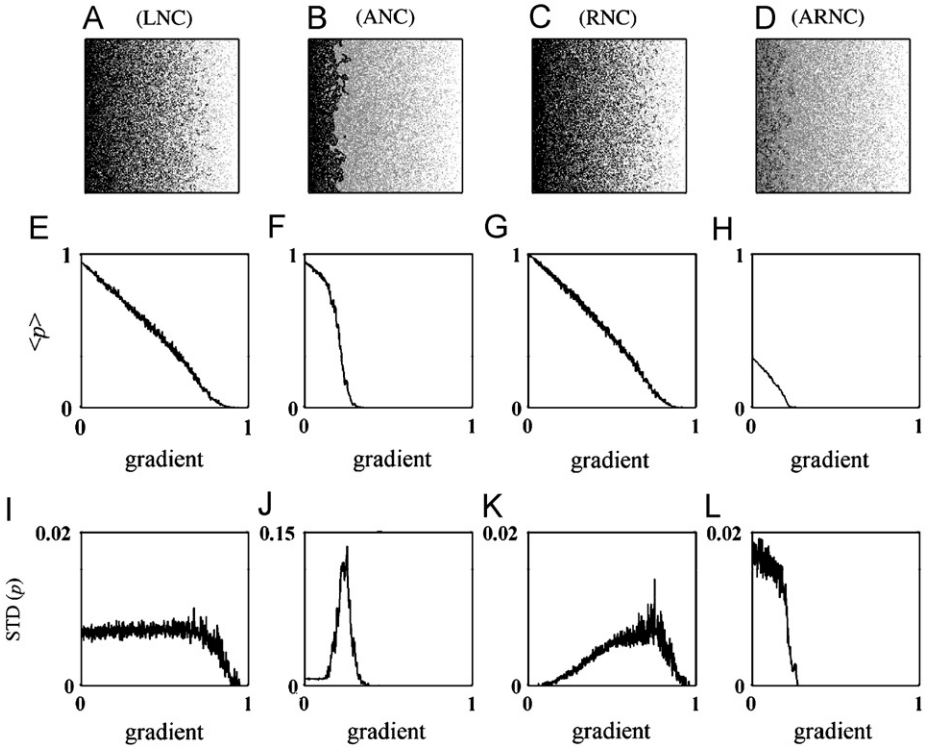

Fig. 4. (A–D) Examples of equilibrial snapshots are shown for the LNC, ANC, RNC and ARNC models experiencing a gradient of decreasing habitat availability from left to right (see text for details; a 256×256 grid size is used for the snapshot plots). Black, gray and white pixels denote, respectively, available and occupied patches, available and empty patches, and unavailable patches. Parameters used are $m = 1$ and $e = 0.05$ (in all models). (E–H) Mean occupancy $\langle p\rangle$, averaged over the vertical transects (and over 200 independent snapshots of size 1000×1000), are plotted along the gradient. (I–L) Standard deviation p (computed over the same 200 snapshots) are plotted along the gradient.

because of the large spatial correlation in the ANC dynamics (noted above), which generates the large fluctuations at the border relative to the other three plots. Interestingly, even though the Rescue metapopulation (RNC) assumes a threshold local extinction rate (expression (4)), both the range limit (Fig. 4C) and the mean occupancy (4G) show similar patterns as does the LNC model. The occupancy fluctuation, however, shows a peak at the range limit as in the Allee metapopulation, but the peak is less sharp and much smaller in magnitude (compare Fig. 4K with J). The occupancy in the Anti-rescue model (ARNC) is overall much less throughout, even at the left end of the gradient where all patches are available (Figs. 4D and H), and the fluctuations quickly drop to negligible levels at the range limit (4L).

6. Discussion

Using neighborhood dispersal in a spatially explicit framework, we have modified the basic colonization and extinction processes in the Levins metapopulation model by incorporating Allee, Rescue and Anti-rescue effects, all operating within the same local neighborhood. We have shown that the overall (landscape-wide) colonization and extinction rates are significantly affected by these local processes, which in turn influence the magnitude, stability and spatial structuring of the equilibrial patch occupancy. Discontinuities in these global rates arise due to the presence of unstable equilibria, which emerge from assumptions about local (per-patch) arrival and extinction rates. This source of instability contrasts with the spatially implicit (mean-field) formulations used in Harding and McNamara (2002), where the unstable equilibrium is built directly into the functional forms of the global rates themselves.

One intriguing effect of localized metapopulation processes that has emerged from our study is that short-term transients can sometimes give a quite misleading impression of the long-term fate of a metapopulation system. This is evident, for instance, in the example shown in Fig. 1C, where the trajectory of the Allee metapopulation starting with a lower initial occupancy first goes up, before it turns around to decline and the metapopulation eventually becomes extinct. Another example showing an opposite trend is depicted in Fig. 2A, where the trajectory of the Rescue metapopulation beginning at the higher initial occupancy first goes down, before it begins to increase and the metapopulation settles into an equilibrium where it persists indefinitely. Understanding transient dynamics in metapopulation is an important challenge for future work, which will need to focus on transient shifts in the structure of spatial covariance in occupancy.

Because of neighborhood dispersal, spatially localized correlations develop among neighboring populations, which are stronger in both the Allee and Rescue metapopulation models than in either the standard Levins or the Anti-rescue models. These differences influence the spatial pattern and distribution of clusters of occupied patches. For example, at comparable levels of patch occupancy, there are more large clusters at equilibrium in the Allee model, and more small clusters in the Anti-rescue model. However, the power-law distribution pattern in the intermediate range of cluster sizes does not appear to depend on the details of local processes. Similar power-laws are known to occur in random percolation models that do not involve any neighborhood interaction (Stauffer and Aharony, 1992; Pascual et al., 2002; Roy et al., 2003; Pascual and Guichard, 2005), and our results buttress the observation that these types of scaling may be a generic feature of the patterns emerging across many kinds of spatial systems. The precise location of the percolation point itself, though, depends on the localized spatial correlation, and in turn, on the nature of local processes, as shown in Fig. 3I.

We have extended our analysis of localized dynamics in a metapopulation to examine the distributional limits of species along environmental gradients. This extends the work of previous authors (Lennon et al., 1997; Holt and Keitt, 2000), who largely considered a simpler class of local processes. We have shown that the localized metapopulation dynamics, when embedded on a smooth gradient of habitat availability, can show significant differences at range limits, depending on the local colonization and extinction processes. For example, the species border is sharpest in the Allee metapopulation model (also see Holt et al., 2005), whereas it is the fuzziest in the Rescue model, comparable to the standard Levins model (compare Fig. 4B with A and C), even though the last two models assume quite different local processes. The patterns of mean occupancy $\langle p \rangle$ along the gradient confirm these results. There are also interesting differences in the standard deviation of occupancies at the range limit, as shown in Figs. 4I–L. These results suggest that the details of localized dynamics may have significant consequences for the spatial structure of range margins.

There are many connections between metapopulation biology and epidemiology. As noted above, the Anti-rescue effect itself can arise from depressed local population sizes due to increased epidemic incidences at high densities. For example, Davis et al. (2004) showed that the risk of bubonic plague outbreaks in metapopulation of great gerbils in Kazakhstan increases with population size. An outbreak in one population can then spillover into neighboring populations, increasing their risk of extinction. By contrast, if once focuses on the initial pattern of spread of an infection, the lower percolation point due to the Allee effect (Fig. 3I) provides a landscape-wide connected pathway at relatively low occupancy levels, which can facilitate disease spread in the metapopulation via neighborhood movements of an infected individual. There may also be evolutionary consequences of the different spatial patterns of occupied patches shown in Figs. 3A–D for host–pathogen interaction. For example, in a highly clustered host population with many gaps between clusters, a virulent locally dispersing pathogen is likely to sweep through a local patch of susceptible hosts, and then die out, more quickly than if the host population is more connected (see also Boots and Sasaki, 1999).

Metapopulation models can also describe systems in which each local "site" contains a single sessile individual in a host population, and each host individual can in turn harbor a population of an infective pathogen. If host individuals are long-lived, and there is no mortality due to infection, then the host population in effect comprises a metapopulation for the pathogen (Hess, 1996; Thrall and Burdon, 1997; Keeling and Gilligan, 2000). For instance, each grid cell could contain an individual tree which could be infected by a fungal pathogen. With this interpretation, the classic Levins metapopulation dynamics, given by Eq. (1), can describe the rate of spread of infection by a specialist pathogen within a spatially distributed host population. We can extend this analogy to our other classes of metapopulation models. For instance, the Allee effect can then emerge from the importance of local propagule size at infection noted in some disease systems, where the infection becomes established in an host individual only if the pathogen load exceeds a minimum threshold, for instance because host defenses are overwhelmed above a certain initial pathogen load (Holt, 2000). Conversely, a Rescue effect may reflect increased rapid re-infection from infected neighbors, preventing clearance of a pathogen by the defense systems of an individual host.

Future work on these models should include, among other things, using different functional forms for the local arrival and extinction rates in the Allee and Rescue models, than the specific threshold forms we assumed in Eqs. (3) and (4). Numerical

evidence suggests that for smaller neighborhood sizes z, A_i should be zero for low n_i (as assumed in Eq. (3)), for an unstable equilibrium to exist in the Allee metapopulation model. As z increases, the dynamics approach that of the global Allee model, and Eq. (3) can be replaced by a smooth function with $A_i > 0$ for all values of n_i. For example, a sigmoid function of the form $A_i = m/[1 + \exp(-n_i + z/2)]$ gives an unstable equilibrium with $z = 24$, but not with $z = 8$ (details not shown). We have also carried out our simulations with different neighborhood sizes, such as $z = 4$ (the "von Neumann" neighborhood) and $z = 24$, and found results that are qualitatively similar to those presented here (with $z = 8$) (details not shown). Furthermore, here we have always assumed that the initial configuration is random placement of occupied sites across the grid. Preliminary analysis suggests that using different initial configurations, such as a square-shaped cluster of occupied patches placed at the center of the grid, or a horizontal (or vertical) strip of such a cluster, but all with same area (same initial occupancy level $p(0)$), does not lead to qualitatively different result (details not shown). However, analysis of potential effects of initial occupancy patterns requires a more thorough examination than we have done to date. Even if initial patterning of occupancy does not influence the long-term equilibrium of a system, it could matter in determining the magnitude and longevity of the interesting transient responses that emerge from localized dynamics.

Acknowledgments

We thank Michael Barfield for useful comments, and National Science Foundation (Grant # EF 0525751) and the University of Florida Foundation for support. K.H. acknowledges the Swedish Research Council and the Centre for Theoretical Biology at Gothenburg University for funding.

Appendix A

A.1. Implementing LNC dynamics

We implement the LNC dynamics on a square grid of size $L = 1000 \times 1000$, and use $z = 8$ (the so-called "Moore" neighborhood) and periodic boundary conditions. (The same L, z and B.C. are used throughout, unless noted otherwise.) Each patch is either empty or occupied depending on the two stochastic processes of extinction and colonization, determined by probabilities $p_C = m/\max(m,e)$ and $p_E = e/\max(m,e)$, where $\max(m,e)$ is the larger of m and e. (These definitions keep p_C and p_E bounded below 1, whereas the rates m and e can be arbitrarily large.) In the asynchronous updating of the grid (to mimic the continuous-time dynamics of Eq. (2)), a random patch i is chosen, and colonization or extinction occurs by the following rules:

1. If i is occupied, a random number r is drawn from a uniform distribution between 0 and 1. If $r < p_E$, i becomes empty; else, nothing happens.
2. Or if i is empty, the number n_i of its occupied neighbors is counted. If $r < p_C n_i/z$, i becomes occupied; else, nothing happens.

Site updates are carried out L times, which constitute a single time unit of the dynamics (this unit should be scaled by $\max(m,e)$ to match the time unit of Eq. (2)). This averages to one update per site per unit of time, independent of the grid size.

A.2. Computing C_{LNC} and E

The colonization rate C_{LNC} in Fig. 1A (solid line plot) is obtained from two separate runs of the LNC dynamics starting with initial random occupancies of 1% and 100%. The two segments of C_{LNC} graph start from the opposite ends of the p-axis (in Fig. 1A) and meet at the intersection point with E, which gives the equilibrium p^*. During these runs, C_{LNC} is numerically computed in each sweep of the grid by averaging $A_i (= mn_i/z)$ over all empty patches, and then multiplying by the factor $1-p$ (following the definition of C_{LNC}). Computation of E follows from the definition $E = ep$.

A.3. Computing the unstable equilibrium p_u^* in Figs. 1C and D

Because of the discontinuity in C_{ANC} at p_u^* (Fig. 1D), it is not possible to determine this equilibrium from the intersection of C_{ANC} and E. Instead, we compute p_u^* by estimating the probability of metapopulation persistence starting with several initial occupancies $p(t = 0)$ near p_u^*. From the definition of p_u^*, we have $p(t \to \infty) = 0$ for $p(0) < p_u^*$, and $p(\infty) = p^*$ for $p(0) > p_u^*$. Thus, the persistence probability, defined as the proportion of 200 independent runs for which $p(t = 10{,}000) > 0$, should jump from 0 to 1 across p_u^*, when plotted against $p(0)$. We determine p_u^* to be the point where this probability equals 0.5, which gives $p_u^* = 0.335$ for the chosen parameter values (Fig. A1). The p_u^* value in the RNC model (Figs. 2A and B) is also computed using this method.

A.4. Computing C_{ANC} and E

Similar to the LNC metapopulation, C_{ANC} is computed by averaging A_i (as defined in Eq. (3)) over all empty patches and then multiplying by the factor $1-p$. Because of the discontinuity at the unstable point p_u^*, C_{ANC} in Fig. 1D is obtained from three separate simulation runs of the ANC dynamics using different initial occupancies: one just below p_u^* (p value at P_1, same as in Fig. 1C) that gives the solid line segment of C_{ANC} between P_1 and $p = 0$, another just above p_u^* (Q_1 as in Fig. 1C) that gives the segment between Q_1 and $p = p^*$, and the final one with 100% initial occupancy that generates the last segment between $p = 1$ and p^*.

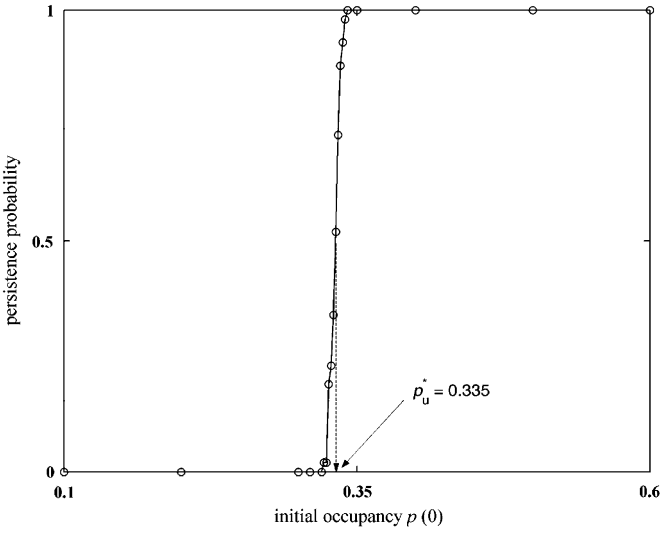

Fig. A1. The probability of metapopulation persistence is plotted against initial occupancy $p(0)$ in the ANC model to determine the unstable equilibrium $p_u^* = 0.335$ (see Appendix A for details). Model parameters are same as in Figs. 1C and D.

Because the initial configurations at P_1 and Q_1 are random (instead of the actual spatially correlated configurations expected near p_u^*), there is a transient period in these two runs before spatial correlations develop and the plots settle onto the underlying (true) colonization function C_{ANC}: these transients are denoted by the segments (P_1,P_2) and (Q_1,Q_2) in C_{ANC}. By contrast, the extinction rate E does not have any discontinuity (except for an insignificant bump at p_u^*), because it is computed by multiplying e and the global density p.

References

Allee, W.C., 1931. Animal Aggregations: A Study in General Sociology. University Chicago Press, Chicago.

Allee, W.C., 1938. The Social Life of Animals. William Heinemann, London.

Amarasekare, P., 1998. Allee effects in metapopulation dynamics. Am. Nat. 152, 298–302.

Boots, M., Sasaki, A., 1999. Small worlds' and the evolution of virulence: infection occurs locally and at a distance. Proc. R. Soc. London Ser. B 266, 1933–1938.

Brown, J.H., Kodric-Brown, A., 1977. Turnover rates in insular biogeography: effect of immigration on extinction. Ecology 58, 445–449.

Courchamp, F., Clutton-Brock, T., Grenfell, B.T., 1999. Inverse density dependence and the Allee effect. TREE 14, 405–410.

Davis, S., Bagon, M., Bruyn, L.D., Ageyev, V.S., Klassovskiy, N.L., Pole, S.B., Viljugrein, H., Stenseth, N.C., Leirs, H., 2004. Predictive thresholds for plague in Kazakhstan. Science 304, 736–738.

Dennis, B., 1989. Allee effects: population growth, critical density, and the chance of extinction. Nat. Resour. Mod. 3, 481–538.

Durrett, R., Levin, S.A., 1994. Stochastic spatial models: a user's guide to ecological applications. Philos. Trans. R. Soc. London B 343, 329–350.

Earn, D.J.D., Levin, S.A., Rohani, P., 2000. Coherence and conservation. Science 290, 1360–1364.

Ellner, S., Fussmann, G., 2003. Effects of successional dynamics on metapopulation persistence. Ecology 84, 882–889.

Gaston, K., 2003. The Structure and Dynamics of Geographic Ranges. Oxford University Press, New York.

Grenfell, B.T., Harwood, J., 1997. (Meta)population dynamics of infectious diseases. TREE 12, 395–399.

Grenfell, B.T., Bolker, B.M., Kleczkowski, A., 1995. Seasonality and extinction in chaotic metapopulations. Proc. R. Soc. London B 259, 97–103.

Guichard, F., Halpin, P.M., Allison, G.W., Lubchenco, J., Menge, B.A., 2002. Mussel disturbance dynamics: signatures of oceanographic forcing from local interactions. Am. Nat. 161, 889–904.

Hanski, I., 1999. Metapopulation Ecology. Oxford University Press, New York.

Hanski, I., Gaggiotti, O.E., 2004. Ecology, Genetics and Evolution of Metapopulations. Elsevier, London.

Harding, K.C., McNamara, J.M., 2002. A unifying framework for metapopulation dynamics. Am. Nat. 160, 173–185.

Harris, T.E., 1974. Contact interactions on a lattice. Annal. Prob. 2, 969–988.

Harrison, S., Taylor, A.D., 1997. Empirical evidence for metapopulation dynamics. In: Hanski, I., Gilpin, M.E. (Eds.), Metapopulation Biology: Ecology, Genetics and Evolution. Academic Press, California, pp. 27–42.

Hastings, A., Harrison, S., 1994. Metapopulation dynamics and genetics. Ann. Rev. Ecol. Syst. 25, 167–188.

Hess, G., 1996. Disease in metapopulation models: implications for conservation. Ecology 77, 1617–1632.

Hinrichsen, H., 2000. Non-equilibrium critical phenomena and phase transitions into absorbing states. Adv. Phys. 49, 815–958.

Holmes, E.E., 1997. Basic epidemiological concepts in a spatial context. In: Tilman, D., Kareiva, P. (Eds.), Spatial Ecology: the Role of Space in Population Dynamics and Interspecific Interactions. Princeton University Press, Princeton, NJ, pp. 111–136.

Holt, R.D., 1993. Ecology at the mesoscale: the influence of regional processes on local communities. In: Ricklefs, R., Schluter, D. (Eds.), Species Diversity in Ecological Communities. University of Chicago Press, pp. 77–88.

Holt, R.D., 2000. A biogeographical and landscape perspective on within-host infection dynamics. In: Bell, C.R., Brylinsky, M., Johnson-Green, P. (Eds.), Proceedings of the 8th International Symposium of Microbial Ecology. Atlantic Canada Soc. Microb. Ecol., Halifax, Canada, pp. 583–588.

Holt, R.D., Keitt, T.H., 2000. Alternative causes for range limits: a metapopulation perspective. Ecol. Lett. 3, 41–47.

Holt, R.D., Keitt, T.H., Lewis, M., Maurer, B., Taper, M., 2005. Theoretical models of species borders: single species approaches. Oikos 108, 18–27.

Hui, C., Li, Z., 2003. Dynamical complexity and metapopulation persistence. Ecol. Model. 164, 201–209.

Hui, C., Li, Z., 2004. Distribution patterns of metapopulations determined by Allee effects. Popul. Ecol. 46, 55–63.

Hurford, A., Hebblewhite, M., Lewis, M.A., 2006. A spatially explicit model for an Allee effect: why wolves recolonize so slowly in Greater Yellowstone. Theor. Popul. Biol. 70, 244–254.

Keeling, M.J., 2002. Using individual-based simulations to test the Levins metapopulation paradigm. J. Anim. Ecol. 71, 270–279.

Keeling, M.J., Gilligan, C.A., 2000. Bubonic plague: a metapopulation model of a zoonosis. Proc. R. Soc. London B 267, 2219–2230.

Keitt, T.H., Lewis, M.A., Holt, R.D., 2001. Allee effects invasion pinning and species borders. Am. Nat. 157, 203–216.

Keymer, J.E., Marquet, P.A., Johnson, A.R., 1998. Pattern formation in a patch occupancy metapopulation model: a cellular automata approach. J. Theor. Biol. 194, 79–90.

Lennon, J.J., Turner, J.R.G., Connell, D., 1997. A metapopulation model of species boundaries. Oikos 78, 486–502.

Levin, S.A., Durrett, R., 1996. From individuals to epidemics. Phil. Trans. R. Soc. London B 351, 1615–1621.

Levin, S.A., Pacala, S.W., 1997. Theories of simplification and scaling in spatially distributed processes. In: Tilman, D., Kareiva, P. (Eds.), Spatial Ecology: the Role of Space in Population Dynamics and Interspecific Interactions. Princeton University Press, Princeton, NJ, pp. 271–295.

Levins, R., 1969. Some demographic and genetic consequences of environmental heterogeneity for biological control. Bull. Entomol. Soc. Am. 15, 237–240.

Lewis, M.A., Kareiva, P., 1993. Allee dynamics and the spread of invading organisms. Theor. Popul. Biol. 43, 141–158.

Marro, J., Dickman, R., 1999. Nonequilibrium Phase Transitions in Lattice Models. Cambridge University Press, Cambridge.

McCarthy, M.A., 1997. The Allee effect, finding mates and theoretical models. Ecol. Model. 103, 99–102.

Oborny, B., Meszéna, G., Szabó, G., 2005. Dynamics of populations on the verge of extinction. Oikos 109, 291–296.

Odum, E.P., 1953. Fundamentals of Ecology, first ed. W.B. Saunders, Philadelphia, PA.

Ovaskainen, O., Sato, K., Bascompte, J., Hanski, I., 2002. Metapopulation models for extinction thresholds in spatially correlated landscapes. J. Theor. Biol. 215, 95–108.

Pascual, M., Guichard, F., 2005. Criticality and disturbance in spatial ecological systems. TREE 20, 88–95.

Pascual, M., Roy, M., Guichard, F., Flierl, G., 2002. Cluster size distributions: signatures of self-organization in spatial ecologies. Philos. Trans. R. Soc. 357, 657–666.

Rohani, P., Lewis, T.J., Grunbaum, D., Ruxton, G.D., 1997. Spatial self-organization in ecology: pretty patterns or robust reality? TREE 12, 70–73.

Rolán-Alvarez, E., Johannesson, K., Erlandsson, J., 1997. The maintenance of a cline in the marine snail *Littorina saxatilis*: the role of home site advantage and hybrid fitness. Evolution 51, 1838–1847.

Roy, M., Pascual, M., Franc, A., 2003. Broad scaling region in a spatial ecological system. Complexity 8, 19–27.

Roy, M., Holt, R.D., Barfield, M., 2005. Temporal autocorrelation can enhance the persistence and abundance of metapopulations comprised of coupled sinks. Am. Nat. 166, 246–261.

Sato, K., Iwasa, Y., 2000. Pair approximation for lattice-based ecological models. In: Dieckmann, U., Law, R., Metz, J.A.J. (Eds.), The Geometry of Ecological Interactions. Cambridge University Press, Cambridge, MA, pp. 341–358.

Snyder, R.E., Nisbet, R.M., 2000. Spatial structure and fluctuations in the contact process and related models. Bull. Math. Biol. 62, 959–975.

Solé, R.V., Bascompte, J., 2006. Self-Organization in Complex Ecosystems. Princeton University Press, Princeton, NJ.

Stauffer, D., Aharony, A., 1992. Introduction to Percolation Theory, second ed. Taylor & Francis, London.

Stephens, P.A., Sutherland, W.J., Freckleton, R.P., 1999. What is the Allee effect? Oikos 87, 185–190.

Thrall, P.H., Burdon, J.J., 1997. Host–pathogen dynamics in a metapopulation context: the ecological and evolutionary consequences of being spatial. J. Ecol. 85, 743–753.

Tilman, D., Kareiva, P., 1997. Spatial Ecology: The role of Space in Population Dynamics and Interspecific Interactions. Princeton University Press, Princeton, NJ.

Wilson, W.G., Nisbet, R.M., Ross, A.H., Robles, C., Desharnais, R.A., 1996. Abrupt population change along smooth environmental gradients. Bull. Math. Biol. 58, 907–922.

Windus, A., Jensen, H.J., 2007. Allee effects and extinction in a lattice model. Theor. Popul. Biol. 72, 459–467.